PAPER 4 (SESSION I)

Stress intensity magnification factors for surface-flawed tension plate and notched round tension bar

Prof A. S. KOBAYASHI* and W. L. MOSS†

* University of Washington, Seattle, Washington, U.S.A.
† North American Rockwell Corporation, Los Angeles, California, U.S.A.

Summary

The stress intensity magnification factor in surface-flawed tension plates is assumed to be decomposable in three parts. The first part of the magnification factor is due to the free front surface, the second part is caused by the free back surface, and the third part is due to the ductility of the material. The first two parts of the magnification factor are derived from published results and the plasticity magnification is based on a modified Dugdale yield zone surrounding a penny-shaped crack in an infinite solid composed of strain hardening material. A semi-elliptical shape surface flaw is replaced by an equivalent penny-shaped crack with the same stress intensity factor and the corresponding plasticity magnification factor is established by estimating the effective crack extension based on the Dugdale model. A procedure for incorporating the effect of through-the-thickness yielding is also proposed. The combined magnification factor is applied to evaluate fracture toughness test results on surface-flawed steel and titanium plates. Also derived is the stress intensity magnification factor due to plasticity in a notched round bar tension specimen. This magnification factor is used to evaluate the fracture toughness of the same steel alloy mentioned above and the results obtained from the two types of specimens are compared.

Introduction

Linear fracture mechanics has gained substantial acceptance in industry during the last decade. Increasing numbers of hardwares are now being designed for fracture prevention and for limited service life where the theory of linear fracture mechanics is used to predict the amount of flaw-growth [1]. This wide application has not only increased the need for stress intensity factor solutions for cracks of realistic geometries but also the need to extend the theory of linear fracture mechanics to structural materials which are somewhat ductile.

One such problem which often confronts a designer of pressure vessels is the problem of deep surface flaws where an analytic solution does not exist for this three-dimensional problem in elasticity. To complicate the matter, the large ductility present in high toughness materials requires an elastic-plastic analysis of this problem. A recent paper by Ayres [2] presents some numerical results of a surface-flawed tension plate loaded close to net-section yield stress but further refinement of such numerical analysis is necessary before a fracture criterion can be derived from such

solution. Thus, the elastic-plastic solution to the problem of deep surface flaw are not immediately in sight at this time.

The object of this paper is to provide an estimate of the stress intensity magnification factor in a deep surface-flawed tension plate composed of somewhat ductile material. Also derived are the plasticity correction factor for a notched round-bar specimen which is often used to evaluate plane strain fracture toughness.

Surface-flawed tension plate

Consider a semi-elliptical surface flaw in a tension plate of finite thickness, t, as shown in Fig. 1 where a and c represent the semi- minor and semi-major diameters of the ellipse, respectively, and σ is the applied uniaxial tension load.

Although no elasticity solution exists for the semi-elliptic surface-flawed tension plate, such solution does exist for an elliptical flaw embedded in an infinite solid and subjected to uniaxial tension. The maximum stress intensity factor for the embedded elliptical flaw can be expressed as [3]

$$K_I = \sqrt{\pi}\,\sigma\,\frac{\sqrt{a}}{\Phi} \tag{1a}$$

where

$$\Phi = \int_0^{\pi/2} \left[1 + \frac{c^2 - a^2}{c^2}\sin^2\theta\right]^{1/2} d\theta \tag{1b}$$

This maximum stress intensity factor is located on the minor axis of the ellipse.

When the elliptical flaw is halved by a free front surface containing the major axis of the ellipse, then equation 1 must be modified to account for the free surface effect. In addition, available result on the semi-infinite solid with a semi-circular surface flaw [4] leads one to believe that the location of maximum stress intensity factor may shift away from the minor axis to the major axis of the semi-elliptical flaw. Countering this effect is the compounding stress intensity factor magnification due to the free back surface in a finite-thickness plate where the stress intensity factor closest to the free back surface is most affected. As a result, the location of maximum stress intensity factor will probably remain on the minor axis of the semi-elliptical surface flaw. Representing the compounded magnification due to the free front and back surface as M_e, equation 1 can be rewritten for surface-flawed tension plates as

$$K_I = M_e\,\sqrt{\pi}\,\sigma\,\frac{\sqrt{a}}{\Phi} \tag{2}$$

When equation 2 is used to evaluate fracture in somewhat ductile material, a further correction due to plasticity must be made. This magnification as proposed by Irwin [3] is obtained by replacing the complete elliptical integral of the second kind, Φ, in equations 1 or 2 by

$$\sqrt{Q} = \left[\Phi^2 - 0{\cdot}212\left(\frac{\sigma}{\sigma_{\text{yield}}}\right)^2\right]^{1/2} \tag{3}$$

where σ_{yield} is the yield stress of the material.

Irwin's ductility correction factor works well for moderate values of $\sigma/\sigma_{\text{yield}}$ but for $\sigma/\sigma_{\text{yield}}$ values approaching or exceeding unity, experimental results show that the apparent fracture toughness computed by the use of equations 2 and 3 becomes suppressed. As a result, the various fracture toughness data obtained by different specimen geometries for the same material can no longer be correlated. A new model of plastic yielding in a surface flaw which provides a stress intensity factor magnification of M_p and which further modifies equation 2 is thus proposed here as follows:

$$K_I = M_e M_p \sqrt{\pi}\,\sigma\,\frac{\sqrt{a}}{\Phi} \tag{4}$$

In the following, each of the magnification factors will be discussed in detail.

Free surface magnification

The magnification due to free front surface has been determined for two extreme cases. For a semi-circular flaw or $a/2c = 0{\cdot}5$, this value is approximately 1·03 [4]. For a single edge-flawed semi-infinite plane or $a/2c = 0$, several investigators [5, 6] have determined this value to be approximately 1·12. Since an analytical solution is not available for $0 < a/2c < 0{\cdot}5$, the following interpolation between the two extreme cases is proposed for representing the effect of the free front surface, M_1*.

$$M_1^* = 1 + 0{\cdot}12\left(1 - \frac{a}{2c}\right)^2 \tag{5}$$

Less is known about the stress intensity factor magnification due to the free back surface. An analogous problem which involves two coplanar parallel elliptical flaws in an infinite solid subjected to uniaxial tension has been solved by the approximate method of point collocation [7]. By bisecting this infinite solid at the plane of symmetry which separates the two coplanar flaws, an approximate solution to the problem of an embedded elliptical flaw near a surface with vanishing shear traction but with residual normal tractions is obtained. The effect of the residual normal tractions is to underestimate the magnification factor for $a/t > 0{\cdot}7$ as shown by similar comparison in plane problems involving the tangent formula and a more

exact analysis [8]. This estimated stress intensity factor magnification, due to the free back surface, is referred to as M_h*.

Assuming no coupling between the magnification factors of the free front and back surfaces, the product of these two factors, M_1* and M_h*, then yields M_e, the elastic magnification factor of the surface-flawed tension plate as shown in Fig. 2.

Fig. 2 shows that the stress intensity factor magnification, M_e, reaches an infinite value as $a/t \to 1$. For a perfectly brittle material, this result is obviously correct but in the presence of plastic yielding an infinite magnification cannot be attained. In order to remove this infinite magnification, it is assumed that the elastic magnification factor, M_e, cannot increase any more, once the plastic yield zone penetrates the thickness of the plate and creates an effective yield hinge. These trucation points of M_e are shown by dashed curves in Fig. 2 for an elastic-perfectly plastic material. Details of the procedure for establishing loads at which the plastic yield zones reach the free back surface are described in the following section.

Plasticity magnification

The commonly used plasticity correction as described previously is a simple but yet effective extension of linear fracture mechanics. Irwin suggested that the effect of plastic yielding can be considered as an effective extension of the crack and estimated this extended crack by the use of the elastic stress field at the crack tip. As mentioned previously, there exists considerable experimental data which support Irwin's simple plasticity magnification for moderate values of applied stress to yield stress ratio.

The method of plasticity correction proposed here is similar to that of Irwin except that a Dugdale model of extended yield zone is used to estimate the amount of effective crack length [9]. This Dugdale model of extended yield zone has been studied for plane problems by Goodier and Field [10] and in considerable detail by Hahn *et al.* [11]. Also the Dugdale model in a penny-shaped crack was studied by Keer and Mura [12].

The Dugdale model for an elliptical crack poses analytical difficulties and therefore the elliptical crack was first replaced by an equivalent penny-shaped crack with the same stress intensity factor. The radius of such penny-shaped crack is represented by

$$b = \left(\frac{\pi/2}{\Phi}\right)^2 a \tag{6}$$

A modified Dugdale model for this equivalent penny-shaped crack with an extended yield zone of linearly varying stress distribution as shown in the inserted schematics of Fig. 3 is then solved. A brief description of this solution is given in Appendix I and therefore only the final results will be discussed in the following.

Consider a cylindrical coordinate system (r, θ, z) with its origin located at the center of the equivalent penny-shaped crack. After removing the stress singularity at the crack tip, the extended crack radius, d, of a Dugdale model can be determined by the following relation.

$$\frac{\sigma}{\sigma_0} = \sqrt{1 - \frac{b^2}{d^2}} + \frac{m}{2\left(1 - \frac{b}{d}\right)}\left[\frac{b}{d}\sqrt{1 - \frac{b^2}{d^2}} - \frac{\pi}{2} + \sin^{-1}\frac{b}{d}\right] \tag{7a}$$

where σ_0 is the maximum uniaxial tensile stress prescribed at the physical crack tip of $r = a$

$$m = 1 - \frac{\sigma_{\text{yield}}}{\sigma_0} \tag{7b}$$

This relation is shown graphically in a more convenient form of b/d versus $\sigma/\sigma_{\text{yield}}$ with m as a parameter in Fig. 3.

The next step is to determine the crack opening displacement (COD) at the center ($r = 0$) of this modified Dugdale crack for the purpose of establishing the crack radius of an equivalent elastic crack to this modified Dugdale crack. The COD close to the physical crack tip of $r = a$ as used by Wells was not used since experimental evidences in analogous two-dimensional problems showed that the COD at the center of the Dugdale crack agreed better with the measured COD [14]. This COD at the center of the equivalent elastic penny-shaped crack is proportional to the square of its stress intensity factor and therefore the magnification factor due to plastic yielding can now be expressed as

$$M_p^2 = \frac{w\,(0,0)]_{\text{Dugdale}}}{w\,(0,0)]_{\text{Elastic}}} = \frac{\sigma_{\text{yield}} \cdot \cos^{-1}\frac{b}{d}}{\sigma(1-m)} + \left[\frac{d}{b} - \frac{\sigma_{\text{yield}}}{\sigma(1-m)}\sqrt{\left(\frac{d}{b}\right)^2 - 1}\right] \tag{8}$$

For ideally plastic material or for $m = 0$, the COD discussed above coincides with the known results of Keer *et al.* [12]. For sake of comparison, plasticity magnification factors are computed and listed together with corresponding M_p values obtained from equations 3 and 8 for ideally plastic material or $m = 0$ and $\sigma/\sigma_{\text{yield}} = 0{\cdot}9$.

	Eq. 8	Eq. 3
Penny-shaped crack	$M_p = 1{\cdot}115$	$M_p = 1{\cdot}035$
Elliptical crack $a/2c = 1$	$M_p = 1{\cdot}115$	$M_p = 1{\cdot}050$

As shown above, the new plasticity magnification factor as computed above is approximately 6–7% larger than the corresponding values obtained by equation 3. Values of M_p for various m values are shown in Fig. 4.

When the plastic yield zone penetrates the thickness of the plate, some modification must be made to account for this penetration. Although the COD will continue to increase with increasing load, the combined stress

intensity magnification factor will reach a maximum value due to excess plastic yielding which will not contribute to the elastic strain energy release rate. In order to account for the topping of the magnification factor, it is proposed that the free surface effect be truncated at values when the modified Dugdale yield zone penetrates the thickness of the plate. The relation for this condition can be easily obtained by the following equation which is derived on geometric considerations only.

$$d = b + t - a \tag{9}$$

This equation together with equations 6 and 7 must be used to solve for the load ratio, σ/σ_{yield}, where such penetration occurs. The dashed curves in Fig. 2 show the relation between a/t, σ/σ_{yield}, and $a/2c$ for elastic, ideally plastic material or $m = 0$. For strain hardening material or $m > 0$, the dashed curves will shift toward the right in Fig. 2 or toward larger values of M_e.

Application of magnification factor

The stress intensity magnification factor for deep surface flaw as derived above was used in evaluating fracture toughness data involving Ladish D6A-C steel and 5 Al-2·5 Sn (ELI) titanium alloy [15, 16]. Figs. 5 and 6 show the fracture toughness results evaluated by the conventional procedure together with the proposed magnification factors. Definite improvement in data correlation is shown in these figures.

These magnification factors were also used to evaluate some unpublished data involving surface-flawed tension plates machined from 5 Al-2·5 Sn (ELI) titanium alloy and tested to fracture at room temperature.* Two of the ten specimens were loaded beyond the 0·2% offset yield strength of the material before fracture. For such data, where the plastic yield zone obviously penetrated through the net section of the specimen, the elastic magnification of M_e at $a/t = 0$ in Fig. 3 was used. For the plasticity magnification factor of M_p, the yield stress σ_{yield}, was equated to the applied stress of σ when σ exceeds the yield strength of the material in computing the strain hardening coefficient of m. Again the data evaluated by the procedure described in this paper showed definite improvement over the data evaluated by the conventional procedure.

Magnification in a notched round bar tension specimen

The magnification factor of stress intensity factor in a notched round bar can also be represented in a form similar to equation 4 as

$$K_I = M_e M_p \sqrt{(\pi)} \sigma_n \sqrt{B} \tag{10}$$

* Test data from Space Branch, The Boeing Company, Seattle, Washington.

where σ_n is the net area stress in the notched round bar
B is the shank diameter of the bar

The elastic magnification factor, M_e, has been estimated by others [8, 17] and therefore will not be elaborated here. The plasticity magnification, M_p, was estimated by applying Wells COD concept to this problem [13], since there exists no convenient reference axis in an external notch with a Dugdale model of extended yield zone. Conceptually, this approach is similar to the method used in the surface-flawed tension plate with the only difference being the position at which the COD was considered. In the notched round bar with a Dugdale model of extended yield zone, the COD at the physical crack tip, $r = b$, $w]_{r=b,\ z=0}$, was then used to establish an equivalent elastic circumferential notch which is deeper than the physical notch. The stress intensity factor of this equivalent notched round bar for an ideally plastic material is

$$K_I^2 = \frac{\mu}{1-\nu} \sigma_{yield} w]_{r=b,\ z=0} \tag{11}$$

where μ is the shear modulus of the material
ν is the Poisson's ratio of the material

The plasticity magnification factor can then be represented as

$$M_p = \frac{K_I]_{\text{Eq. 11}}}{\frac{\sqrt{\pi}}{2\sqrt{2}} \sigma_n \sqrt{b}} \tag{12}$$

This relation is shown in Fig. 7 for an ideally plastic material or $m = 0$.

These magnification factors were then used to evaluate the experimental data of notched round bars machined out of the same Ladish D6A-C steel used for the surface-flawed specimens described previously [15]. The averaged values of the test results for the fifteen specimens are shown in the following:

$B = 0{\cdot}501$ in
$b = 0{\cdot}333$ in notch diameter after fatigue loading
$\sigma_n = 156{\cdot}5$ ksi

$M_e = 0{\cdot}240$ for $\frac{b}{B} = 0{\cdot}665$ (Ref. 8)

$M_p = 1{\cdot}06$ for $\frac{\sigma_n}{\sigma_{yield}} = 0{\cdot}633$ (Fig. 7)

The resultant fracture toughness computed by equation 10 is

$$K_{Ic} = 50{\cdot}0 \text{ ksi } \sqrt{\text{in}}$$

This value compares favorably with the average fracture toughness of 49·8 ksi determined by the data of surface-flawed specimens illustrated in Fig. 5.

Conclusions

Stress intensity magnification factors for surface-flawed tension plate and notched round tension bar have been derived. In the limited applications cited here the proposed magnification factors show definite improvement over the conventional correction factors.

Acknowledgement

The research work reported in this paper was supported by the Space Branch of The Boeing Company and in parts by the Space Branch of the North American Rockwell Company.

References

1. TIFFANY, C. F. and MASTERS, J. N. 'Applied fracture mechanics'. *Amer. Soc. Testing Materials*, STP381, . pp. 249-278, June, 1964.
2. AYRES, D. J. 'A numerical procedure for calculating stress and deformation near a slit in a three-dimensional elastic-plastic solid'. *NASA Tech. Memo.* X-52440, 1968.
3. IRWIN, G. R. 'Crack extension force for a part-through crack in a plate'. *J. of Applied Mechanics, Trans. of ASME*, vol. 29, Series E, pp. 651-654, December, 1962.
4. SMITH, F. W., EMERY, A. F. and KOBAYASHI, A. S. 'Stress intensity factors for semi-circular cracks, part II'. *J. of Applied Mechanics, Trans. of ASME*, vol. 34, Series E, no. 4, pp. 952-959, December, 1967.
5. WIGGLESWORTH, L. A. 'Stress distribution in a notched plate'. *Mathematika*, vol. 4, pp. 76-96,1957.
6. BOWIE, O. L. 'Rectangular tensile sheet with symmetric edge cracks'. *J. of Applied Mechanics, Trans. of ASME*, vol. 31, Series E, no. 2, pp. 208-212, June, 1964.
7. KOBAYASHI, A. S., ZIV, M. and HALL, L. R. 'Approximate stress intensity factor for an embedded elliptical crack near two parallel free surfaces'. *Int. J. of Fracture*, vol. 1, no. 2, pp. 81-95, 1965.
8. PARIS, P. C. and SIH, G. C. 'Stress analysis of cracks'. *Amer. Soc. Testing Materials*, STP381, pp. 30-81, June, 1964.
9. DUGDALE, D. S. 'Yielding of steel sheets containing slits'. *J. of Mech. and Physics of Solids*, vol. 8, pp. 100-104, 1960.
10. GOODIER, J. N. and FIELD, F. A. 'Plastic energy dissipation in crack propagation'. *Fracture of Solids*, editor Gilman and Drucker, John Wiley, pp. 103-118, 1963.

11. ROSENFIELD, A., DAI, P. K. and HAHN, G. T. 'Crack extension and propagation under plane stress'. *Proc. of 1st Intl. Conf. on Fracture* (Sendai), pp. 223-258, September, 1965.
12. KEER, L. M. and MURA, T. 'Stationary crack and discontinuous distributions of dislocations'. *Proc. of the 1st Intl. Conf. on Fracture* (Sendai), pp. 99-116, September, 1965.
13. WELLS, A. A. 'Application of fracture mechanics at and beyond general yielding'. *British Welding J.*, vol. 81, pp. 563-570, 1963.
14. KOBAYASHI, A. S., ENGSTROM, W. L. and SIMON, B. R. 'Crack-opening displacements and normal strains in centrally-notched plates'. To be published in *J. of Experimental Mechanics*.
15. TIFFANY, C. F. and LORENTZ, P. M. 'An investigation of low cycle fatigue failures using applied fracture mechanics'. Air Force Materials Laboratory Report ML-TDR-64-53, May, 1964.
16. TIFFANY, C. F., LORENTZ, P. M. and HALL, L. R. 'Investigation of plane-strain flaw growth in thick-walled tanks'. NASA CR-54837, February, 1966.
17. HARRIS, D. O. 'Stress intensity factors for hollow circumferentially notched round bars'. *J. of Basic. Eng., Trans. of ASME*, vol. 89, Series D, no. 1, pp. 49-54, March, 1967.
18. MOSSAKOVSKII, V. I. and RYBKA, M. T. 'Generalization of the Griffith-Sneddon criterion for the case of a nonhomogeneous body'. *PMM*, vol. 28, no. 6, pp. 1277-1286, 1964.

Appendix I: Solution for modified Dugdale model in a penny-shaped crack

Consider a penny-shaped crack embedded in an infinite elastic solid which is subjected to a uniform tensile stress, σ, perpendicular to the plane of the crack. The normal stress component in the Dugdale model of extended yield zone is assumed to vary linearly from a maximum value of σ_0 at the edge of the physical crack to a minimum value of σ_{yield} at the edge of the extended crack. The origin of a cylindrical coordinate system (r, θ, z) is assumed to be located at the center of the crack. Because of symmetry it is sufficient to consider the half-space $z = 0$ which is subjected to the mixed boundary conditions of

$$\tau_{rz}(r, 0) = 0 \qquad \text{for all } r \qquad \text{(I.1a)}$$

$$\sigma_{zz}(r, 0) = -\sigma \qquad 0 < r < b \qquad \text{(I.1b)}$$

$$= \sigma_0[1 - m_1 (r - b)] - \sigma \qquad b < r < d \qquad \text{(I.1c)}$$

$$w(r, 0) = 0 \qquad d < r < \infty \qquad \text{(I.1d)}$$

where

$$m_1 = \frac{m}{d - b} \qquad \text{(I.1e)}$$

It is easily shown that when the stresses and displacements are expressed in terms of Hankel transforms, the resulting boundary conditions for the axisymmetric problem may be written as

$$\sigma_{zz} = \frac{\mu}{1-\nu}\frac{\partial F(r,0)}{\partial z} = -\sigma \qquad 0 < r < b \qquad \text{(I.2a)}$$

$$= \sigma_0 [1 - m_1 (r-b)] - \sigma \qquad b < r < d \qquad \text{(I.2b)}$$

$$w(r,\ 0) = F(r,\ 0) = 0 \qquad d < r < \infty \qquad \text{(I.2c)}$$

where
$$F(r,\ z) = \int_0^\infty \psi(\xi)\, e^{-\xi z} J_0(r\xi)\, d\xi \qquad \text{(I.2d)}$$

Following Mossakovskii and Rybka [18] the harmonic function $W(x,\ z)$ is defined as

$$W(x,z) = \int_0^\infty \frac{\psi(\xi)}{\xi} \sin(\xi x)\, e^{-\xi z}\, d\xi \qquad \text{(I.3)}$$

Then, by representing $J_0(r\xi)$, $\xi J_0(r\xi)$ and $\sin \xi x/\xi$ by their Mellin transformations, we obtain

$$\int_0^x \frac{\partial F}{\partial z}(r,z)\frac{r\,dr}{\sqrt{x^2-r^2}} = \frac{\partial W}{\partial z}(x,z) \qquad \text{(I.4a)}$$

$$\frac{\partial}{\partial x}\int_x^\infty F(r,z)\frac{r\,dr}{\sqrt{r^2-x^2}} = \frac{\partial W}{\partial z}(x,z) \qquad \text{(I.4b)}$$

$$\frac{\partial}{\partial r}\int_0^r \frac{\partial W}{\partial z}\frac{x\,dx}{\sqrt{r^2-x^2}} = \frac{\pi r}{2}\frac{\partial F}{\partial z}(r,z) \qquad \text{(I.4c)}$$

$$\int_r^\infty \frac{\partial W}{\partial z}\frac{dx}{\sqrt{x^2-r^2}} = -\frac{\pi}{2}F(r,z) \qquad \text{(I.4d)}$$

The preceding transformations illustrate the relationship between the three-dimensional axisymmetric function $F(r,\ z)$ and the two-dimensional function $W(x,\ z)$. When combined with equations I.2a, I.2b and I.2c, the normal stress $\sigma(r,\ 0)$ and the normal displacement $w(r,\ 0)$ are completely defined when the function $W(r,\ 0)$ has been determined. It is easily shown that all the stresses and displacements in the three-dimensional body are defined when the function $W(x,\ z)$ is defined. However, it is not necessary to determine $W(x,\ z)$ for the problem being considered.

When the boundary conditions are substituted into equations I.4a and I.4b and the indicated operations performed, we obtain

$$\sigma_z(r,0) = \frac{\mu}{1-\nu}\frac{\partial F}{\partial z} = \frac{2}{\pi}\left[\sigma\left\{\frac{d}{\sqrt{r^2-d^2}} - \sin^{-1}\frac{d}{r}\right\} + \sigma_0\left\{\left(1+\frac{m_1 b}{2}\right)\left(-\sqrt{\frac{d^2-b^2}{r^2-a^2}}\right.\right.\right.$$
$$+ \sin^{-1}\sqrt{\frac{d^2-b^2}{r^2-d^2}}\Bigg) - \frac{M}{2}\left[\left(\frac{\pi}{2} - \sin^{-1}\frac{b}{d}\right)\left(\frac{d^2}{\sqrt{r^2-d^2}} - 2\sqrt{r^2-d^2}\right)\right.$$
$$+ \frac{4b}{3}\tan^{-1}\sqrt{\frac{r^2-d^2}{d^2-b^2}} - 2r\cot^{-1}\frac{b}{r}\sqrt{\frac{r^2-d^2}{d^2-b^2}} - \frac{2\pi b}{3} + \pi r$$
$$\left.\left.\left.+ \frac{b}{3}\sin^{-1}\sqrt{\frac{d^2-b^2}{r^2-b^2}}\,2\right]\right\}\right] \qquad r \geq d \qquad \text{(I.5a)}$$

$$w(r,0) = \frac{4}{\pi}\frac{(1-\nu^2)\,\sigma}{E}\left\{\sqrt{d^2-r^2} + \frac{\sigma_0}{\sigma}\left(d\sqrt{\frac{d^2-b^2}{d^2-r^2}} - b\,E\left(u,\frac{r}{b}\right)\right)\right\} \qquad \text{(I.5b)}$$

where $u = \sin^{-1}\sqrt{\dfrac{d^2-b^2}{d^2-r^2}}$

The normal stress will be finite at $r = d$ when

$$\frac{\sigma}{\sigma_0} = \sqrt{1-\frac{b^2}{d^2}} + \frac{m}{2\left(1-\frac{b}{d}\right)}\left[\frac{b}{d}\sqrt{1-\frac{b^2}{d^2}} - \frac{\pi}{2} + \sin^{-1}\frac{b}{d}\right] \qquad \text{(I.5c)}$$

$$m = 1 - \frac{\sigma_{\text{yield}}}{\sigma_0}$$

Appendix II: Solution for a Dugdale model in an external circular crack

This appendix outlines a procedure for computing the plasticity magnification factor for a Dugdale model in infinite elastic solid which contains an external circular notch in the region of $b \leq r$ and $z = 0$. A constant load, P, perpendicular to the plane of the notch, is applied to the solid at $z = +0$.

In order to solve this problem with the method presented in Appendix I, it is necessary to use the correlation between the notch and the die problem. The elastic problem will be used to illustrate this correlation. The boundary conditions for the elastic problem are:

$$w(r,\ 0) = F(r,\ 0) = \epsilon \qquad 0 < r < b \qquad \text{(II.1a)}$$

$$\sigma_{zz}(r,0) = \frac{\mu}{1-\nu}\frac{\partial F}{\partial z} = 0 \qquad b < r \qquad \text{(II.1b)}$$

Following the procedure outlined in Appendix I, $F(r, z)$ and $W(x, z)$ are represented by equations I.2d and I.3, respectively. Then it is easy to derive the following transformations:

$$\frac{\partial}{\partial x}\int_0^x \frac{F(r,z)\,r\,dr}{\sqrt{x^2-r^2}} = \frac{\partial W}{\partial x}(x,z) \qquad \text{(II.2a)}$$

$$\int_x^\infty \frac{\partial F}{\partial z}\frac{r\,dr}{\sqrt{r^2-x^2}} = -\frac{\partial W}{\partial x}(x,z) \qquad \text{(II.2b)}$$

$$\int_0^r \frac{\partial W}{\partial x}\frac{dx}{\sqrt{r^2-x^2}} = \frac{\pi}{2}F(r,z) \qquad \text{(II.2c)}$$

$$\frac{\partial}{\partial r}\int_r^\infty \frac{\partial W}{\partial x}\frac{x\,dx}{\sqrt{x^2-r^2}} = \frac{\pi r}{2}\frac{\partial F}{\partial z} \qquad \text{(II.2d)}$$

When the appropriate boundary conditions are substituted into the preceding equations, we obtain

$$\sigma_{zz} = \frac{\mu}{1-\nu}\frac{2}{\pi}\frac{\epsilon}{\sqrt{b^2-r^2}} \qquad \text{(II.3)}$$

In order to evaluate ϵ, the total load applied to the bar is denoted by P. Then

$$P = \int_0^b\int_0^{2\pi} \sigma_{zz}\, r\, d\theta\, dr \qquad \text{(II.4a)}$$

$$= \frac{4\epsilon b\mu}{1-\nu}$$

Therefore

$$\epsilon = \frac{1-\nu}{4b\mu}P \qquad \text{(II.5a)}$$

and

$$\sigma_{zz} = \frac{P}{2\pi b}\frac{1}{\sqrt{b^2-r^2}} \qquad \text{(II.5b)}$$

which agrees with the well known results for an external notch.

The boundary conditions for the Dugdale model are

$$w(r,\,0) = F(r,\,0) = \epsilon \qquad 0 < r < a \qquad \text{(II.6a)}$$

$$\sigma_{zz}\,(r,0) = \frac{\mu}{1-\nu}\frac{\partial F}{\partial z} = \sigma_{\text{yield}} \qquad a < r < b \qquad \text{(II.6b)}$$

$$= 0 \qquad b < r \qquad \text{(II.6c)}$$

Substitution of the preceding boundary conditions into equations II.2a and II.2b results in

$$\sigma_{zz} = \frac{\mu}{1-\nu}\frac{\partial F}{\partial z}(r,0) = \frac{\mu}{1-\nu}\frac{2}{\pi}\left[-\frac{\epsilon}{\sqrt{a^2-r^2}} + \sigma_{\text{yield}}\left\{-\frac{\sqrt{b^2-a^2}}{2\sqrt{a^2-r^2}} - \frac{\pi}{2}\right.\right.$$

$$\left.\left. + \sin^{-1}\sqrt{\frac{a^2-r^2}{b^2-r^2}} - \frac{1}{2}\frac{(b^2-r^2)}{\sqrt{(b^2-a^2)(a^2-r^2)}} + \frac{1}{2}\frac{a^2-r^2}{\sqrt{b^2-a^2}}\right\}\right] \qquad \text{(II.7)}$$

Consequently the stresses will be finite at $r = 0$ if

$$\epsilon + \sigma_{\text{yield}}\sqrt{b^2-a^2} = 0 \qquad \text{(II.8)}$$

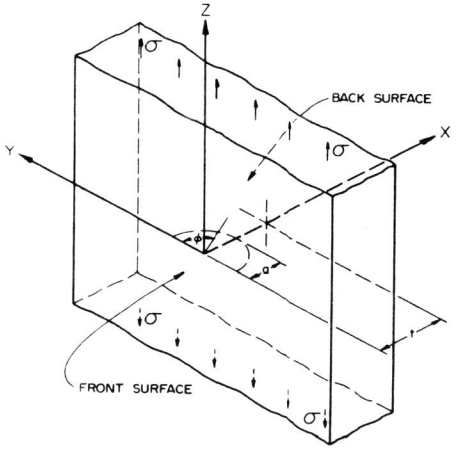

Fig. 1. Semi-elliptical surface flaw in a plate subjected to uniaxial tension.

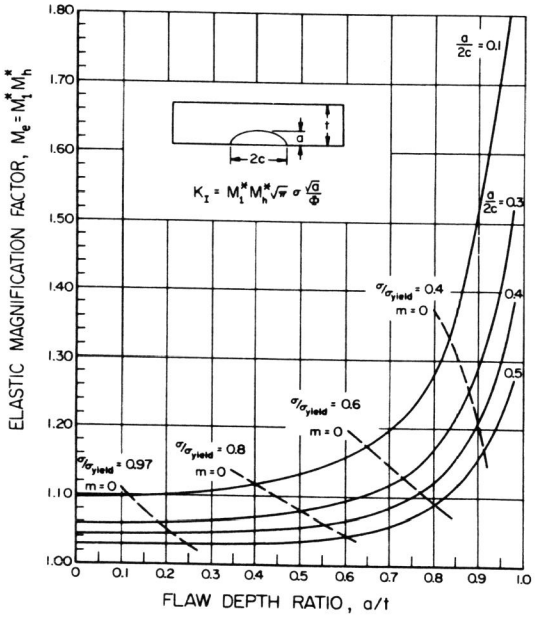

Fig. 2. Elastic stress intensity magnification factor, M_e, for a surface-flawed tension plate.

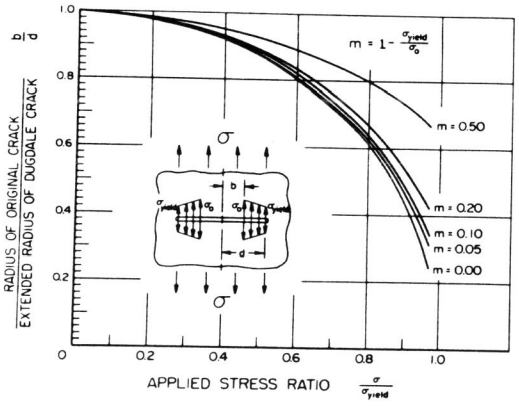

Fig. 3. Extended radius of a penny-shaped crack with Dugdale type yield zone in an infinite solid subjected to uniaxial tension.

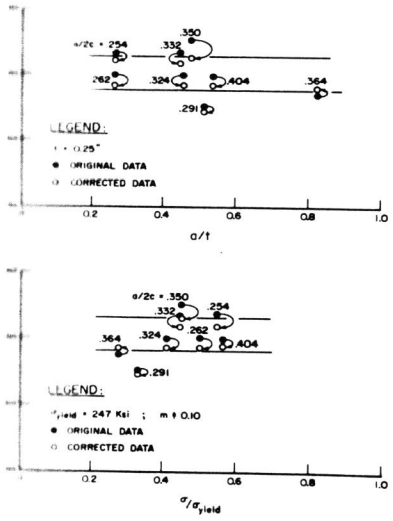

Fig. 5. Ladish D6A-C steel plate at room temperature. [15]

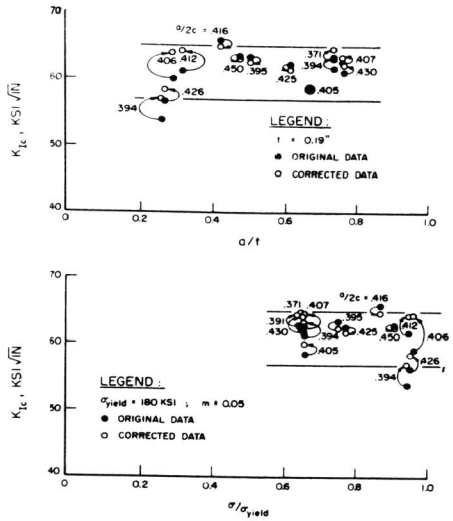

Fig. 6. 5A1-2.5 Sn (ELI) titanium at −320° F [16].

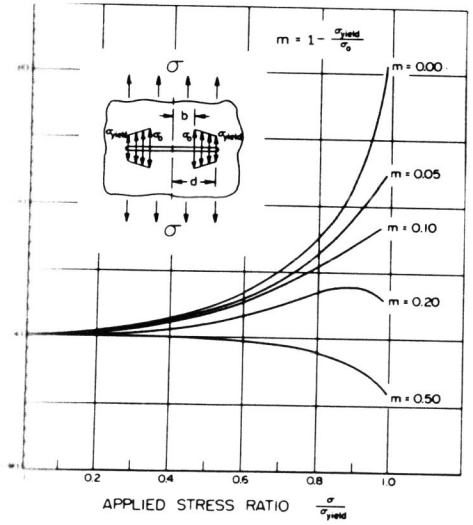

Fig. 4. Plasticity stress intensity magnification factor for penny-shaped crack in an infinite solid subjected to uniaxial tension.

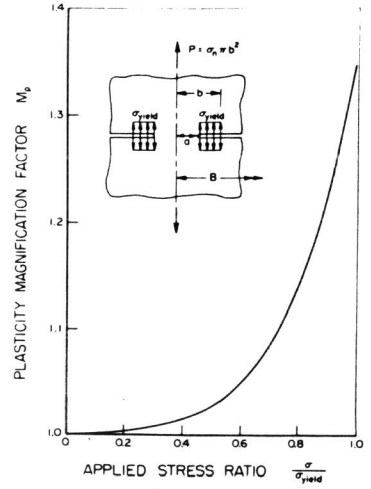

Fig. 7. Plasticity magnification factor for notched round tension bar.